

Thermal Stress Analysis of Annular Fin Subject To Varying Contact Pressure and Heat Conduction

Hsin-Yi Lai*, Jen-Hung Wei**
Kuei-Hao Chang***, Chao-Kuang Chen*

Keywords : Thermal contact conductivity, contact pressure, heat transfer, thermal stress, annular fin

ABSTRACT

The purpose of this paper is to investigate the heat transfer and thermal stress of a variable temperature inner tube for transporting saturated water vapor and its external interference annular fin under different contact pressures. The related variables include interference between the fin and the inner tube, the fin material and fin radius ratio, to obtain temperature and thermal stress distribution under different variables, as well as possible damage beyond the design limit, to confirm that the system can operate within the scope of safety design.

First, the contact pressure between the two interfaces is obtained by considering the temperature boundary condition of the inner tube wall varying with time and the saturated vapor pressure at that temperature. Subsequently, contact thermal conductivity is calculated by Yovanovich's empirical formula, and then the thermal contact conductivity is used as the boundary condition of the fin to solve the temperature distribution curve. The distribution curve of thermal stress, including radial stress and tangential stress, is obtained from the temperature field.

In this paper, the effects of various interferences and different ratios of fin diameters on temperature distribution, temperature difference at the interface, and thermal stress distribution of fins are discussed, as is the relationship between heat transfer efficiency and heat transfer capacity of fins in a steady state.

Paper Received June, 2020. Revised September, 2020, Accepted October, 2020, Author for Correspondence: Chao-Kuang Chen.

* Professor, Department of Mechanical Engineering, National Cheng-Kung University, Tainan, Taiwan, ROC.

** Graduate Student, Department of Mechanical Engineering, National Cheng-Kung University, Tainan, Taiwan, ROC.

*** Associate Research Fellow, Innovation Headquarters, Tainan, Taiwan, ROC.

conductivity, while contact thermal conductivity affects the heat transfer efficiency of fins. The temperature disparity on the contact surface decreases with the increase in contact pressure. The interference can effectively narrow the temperature gap, and the stress field varies with the interference, the ratio of inner to outer radius, and the thermal expansion rate of the material itself. The greater the interference, the greater the radial stress near the contact surface, and the circumferential stress distribution is transformed from the pressure on the fin base to the tensile force at the fin tail end. This is because, when the effect of temperature change is less than that of displacement, the circumferential stress will present compressive force and vice versa; it will present tensile force. The greater the ratio of inner to outer diameter, the greater the stress in the circumference and radial direction.

INTRODUCTION

With the rapid development of science and technology, there are many kinds of scientific and technological products in our lives, such as mobile phones and airplanes. The operation of machines is usually accompanied by the success rate of energy conversion and the waste heat generated in the process. When excessive waste heat may lead to the destruction of working equipment, the parts will be deformed due to residual thermal stress, in addition to some of them. Functions cannot play outside a forced operation, resulting in extrusion collision, so no matter what kind of heat dissipation to each structure occurs, it is an important issue.

The most basic structures of heat dissipation components, such as heat dissipation fins, also evolve from basic rectangular fins to meet various needs and produce a range of fin shapes, such as spiral fins, pin fins, circular fins, etc. The principle is that heat is transferred from the heating equipment to the external environment of its low temperature with heat conduction, heat convection and heat radiation, and the heat will continue to transfer until there is no temperature difference between the substances.

Without changing the structure, improving heat dissipation efficiency, using good thermal conductive materials, and increasing the heat dissipation area of the structure can improve heat transfer.

Annular fins, as an effective and cheap means to enhance heat transfer, have been widely used in various fields, including fins on air-cooled heat exchanger air fin tubes or electronic components. According to the processing technology, they can be subdivided into suit fins and spiral fins. The technology of the set fin is the simplest and earliest processing method. The equipment used is cheap and easy to maintain. The set fin is a single fin processed by a punching machine and fitted on the tube bundle according to a certain interference. There is always a certain contact thermal resistance at the base of the fin. Therefore, when the fin is not installed properly or operated for a long time, due to thermal stress and other effects, the pre-tightening force may disappear and form a gap, resulting in increased contact thermal resistance, which will lead to a great impact on the fin's heat dissipation.

There are many kinds of heat conduction analysis of annular fins. Among them, Aziz (1975) calculated the analytical solutions of annular rectangular fins with periodic temperature changes on the fin base, and the temperature distribution and convection parameters is compared with fin efficiency in disparate periods. Yovanovich(1988) deduced the steady-state solution of two-dimensional isotropic annular fins and compared the fin efficiency of one-dimensional numerical modeling and two-dimensional fins under varying boundary conditions. Ullman and Kalman (1989) derived the fin efficiency and the optimal size of the annular fin under assorted cross sections using the numerical method. Look (1997) proposed a correction term based on the governing equation of fin tip temperature. Moreover, in the thermal convection environment, the fin tip should be assumed to be insulated. The expressions of the validity of one-dimensional and two-dimensional fins were also proposed. Yu and Chen (1999) used the Taylor transformation method and finite-difference approximation method to deduce the transient temperature field of a circular rectangular fin with a temperature gradient change on the fin base, and consider the heat transfer term and heat convection and radiation at the tip of the fin. Shuja et al. (1999) used algebraic software to calculate the optimal heat transfer size of fins in a steady state with a heat source, convection coefficient, and radiation coefficient as variables. Mustafa(2011) deduced the analytical solution of two-dimensional orthotropic materials and considered contact thermal resistance. The results were compared with the dimensions and operation parameters of one-dimensional modeling.

Relevant thermal stress analyses of annular fins include Wu (1997), who calculated the radial and

circumferential thermal stress distribution of annular fins under transient conditions by Laplace transformation. Chiu and Chen (2002) used the ADM method to calculate the stress field of annular fins in a steady state with varying heat conductivity, and considered the heat convection and radiation terms. The temperature field and the stress field of annular fins in a steady state under the periodic variation of the base temperature were considered by the same method every other year. Jabbari et al. (2002) used the semi-analysis method to explore how different stress conditions exerted on annular fins under varying cross sections would affect the distribution of thermal stress fields. Other numerical methods include the finite difference method, finite element method, Runge-Kutta method, homotropy method, and differential transformation method.

The review of the above literature reveals that the analysis of annular fins has made considerable contributions. The general categories of annular fins include steady-state or transient, one-dimensional or two-dimensional, whether one considers contact thermal conductivity, heat transfer analysis, thermal stress analysis, etc. However, at present, the way to consider contact thermal conductivity is limited to using the lumped method to package all variables. Installed in this way, it can-not be seen that the actual contact thermal conductivity is related to the temperature difference on the contact surface, that is, the sudden drop in temperature when heat is transferred from the inner tube bundle to the fin.

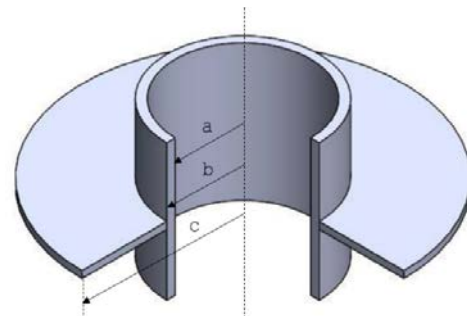


Fig. 1. Annular fin structure model

This study is based on the consideration of the contact thermal resistance between the fin and the inner tube. Considering Yovanovich's empirical formula of contact pressure and thermal conductivity, the finite element method is used to simulate the stress and temperature fields in the case of non-contact thermal resistance and contact thermal resistance. The effects of different tolerances and materials on the stress and temperature fields in the case of thermal resistance are discussed, and the relevant trends are summarized. The geometry of this study is shown in Fig. 1. Because of its axisymmetric nature, it can be simplified to Fig. 2. The dimension design is shown in Table 1. The inner tube is made of structural steel, while the fin is made of copper alloy

and aluminum alloy. The material properties are shown in Table 2.

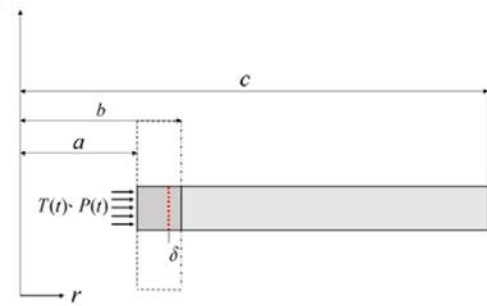


Fig. 2. Annular fin for a one-dimensional mode

Table 1. Model Size Table

Tube inner radius a	45 mm
Tube outer radius b	50 mm
Fin outer radius c	100 mm
Interference δ	Variable

Table 2. Material property

	Structure steel	Copper alloy	Aluminum alloy
E(Gpa)	200	110	71
ν	0.3	0.34	0.33
$\alpha(10^{-6}/K)$	1.2e-5	1.8e-5	2.3e-5
k(W/mK)	60.5	401	166
$C_p(J/kg \cdot K)$	434	385	875
$\rho(kg/m^3)$	7850	8300	2770

ANALYSIS

First, the related theories in this paper are introduced, which are divided into the contact pressure calculation formula, contact thermal conductivity introduction, and semi-empirical formula.

Contact pressure

The contact pressure between the inner tube and the fin when calculating to contact heat conduction. The initial contact pressure between the inner tube and the fin can be calculated using this formula :

$$p = \frac{\delta}{b \left[\frac{1}{E_h} \left(\frac{c^2 + b^2}{c^2 - b^2} + \nu_h \right) + \frac{1}{E_i} \left(\frac{b^2 + a^2}{b^2 - a^2} + \nu_i \right) \right]} \quad (1)$$

Alternatively, the Add Offset function can be used in the package software ANSYS. Contact pressure between the contact faces when simulating an interference fit.

Thermal contact conductance

The transfer of heat between materials is limited to a few channels under a limited contact area, which also makes the temperature distribution at the interface more complex and three-dimensional. An effective assumption for complex temperature fields is that there is a temperature difference between interfaces. That is, the temperature field is discontinuously distributed, and the temperature is proportional to the heat flux passing through. A proportional constant is called *contact thermal conductivity* h_c , and the reciprocal of contact thermal conductivity is contact thermal resistance R_c , according to the interface. The temperature drops and the heat flux passed through are defined as

$$h_c = \frac{1}{R_c} = \frac{q''}{\Delta T} \quad (2)$$

Each rough bump at the interface can be seen as a tiny indenter pressed into a relatively soft material, so the applied pressure is critical for micro-hardness, and microscopically, the area of actual contact is miniscule. Therefore, the average pressure caused by the contact surface is actually much larger than the defined pressure, which also raises a problem: the high-strength stress is applied to the rough contact surface as either an elastic contact or a plastic contact.

Some specific parameters are currently included in the semi-empirical formula developed, which are used extensively in the estimation of contact thermal conductance, including the effective heat transfer coefficient K_s , roughness and slope on a rough surface, and the root mean square values, as shown in Figure 3, which are defined as follows:

$$K_s = \frac{2K_1K_2}{K_1 + K_2} \quad (3)$$

$$\sigma_s = \sqrt{\sigma_1^2 + \sigma_2^2} \quad (4)$$

$$m_s = \sqrt{m_1^2 + m_2^2} \quad (5)$$

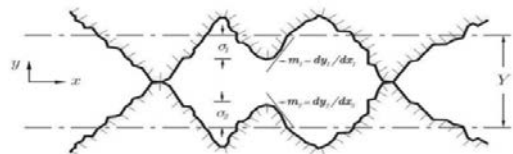


Fig. 3. Microscopic schematic of the contact interface

The plasticity index γ was developed using Mikic(1974) as a criterion for determining elastic deformation or deformation. It is defined as

$$\gamma = \frac{H_{mic}}{E m_s} \tag{6}$$

where H_{mic} represents the micro-hardness of the softer material, E represents the effective Young's modulus, and m_s represents the root mean square of the slope on the rough surface. The condition for determining the deformation between the interfaces is

$$\frac{1}{E} = \frac{1-\nu_1^2}{E_1} + \frac{1-\nu_2^2}{E_2} \tag{7}$$

when the contact between the interfaces of $\gamma \geq 3$ is elastic deformation, as in $\gamma \leq 0.33$ is plastic deformation. Taking the interface property parameters into equation (6), as shown in Table 3. It can be seen that the contact model belongs to the plastic contact model.

There are many kinds of precision that affect the empirical formula, including material properties, interface properties, and media for contact gaps. The empirical formula for plastic contact allowed in this paper is defined by the Yovanovich correlation (1984).

$$h_c = 1.25 \frac{k_s m_s}{\sigma_s} \left(\frac{P}{H_c} \right)^{0.95} \tag{8}$$

The author's evaluation of formula (8) can be used for multiple sets of experimental data in early years. The scope of application is $10^{-6} < P/H_c < 2.2 \times 10^{-2}$.

Table 3. Interface property

	σ_s [17]	m_s (2005)	H_{mic} (2005)	E	ν
Al	5.52 (μm)	0.22	1.089 (Gpa)	71 (Gpa)	0.33
Cu	2.68 (μm)	0.16	0.912 (Gpa)	110 (Gpa)	0.3

GOVERNING EQUATIONS

This paragraph concerns the system heat transfer system equation and stress system equation, as well as the boundary conditions of temperature and stress.

The equilibrium equation of transient, one-dimensional heat transfer equation and plane stress two-dimensional can be expressed as:

Heat Transfer Equation

$$\frac{1}{r} \frac{\partial}{\partial r} \left(kr \frac{dT}{dr} \right) - 2h(T - T_\infty) = \rho c_p \frac{\partial T}{\partial t} \tag{9}$$

Equilibrium Equation

$$\frac{d\sigma_{rr}}{dr} + \frac{1}{r}(\sigma_{rr} - \sigma_{\theta\theta}) = 0 \tag{10}$$

$$\frac{d^2u}{dr^2} + \frac{1}{r} \frac{du}{dr} - \frac{u}{r^2} = (1+\nu)\alpha \frac{dT}{dr} \tag{11}$$

Temperature Boundary Condition

$$T(a,t) = \begin{cases} 100 + 5t, & 0 \leq t \leq 20 \\ 200 & \end{cases} \tag{12}$$

$$-k \frac{\partial T(b,t)}{\partial r} = h(T_b - T(b,t)) \tag{13}$$

$$\frac{\partial T(c,t)}{\partial r} = 0 \tag{14}$$

Stress Boundary Condition

$$\sigma_i(a,t) = -P(t) \tag{15}$$

$$\sigma_i(b,t) = \sigma_h(b,t) \tag{16}$$

$$u_i(b,t) - u_h(b,t) = \delta \tag{17}$$

$$\sigma_h(c,t) = 0 \tag{18}$$

$P(t)$ is defined as

$$P(t) = \begin{cases} 101350 + 18147.5t + 1316.417t^2 + 52.3t^3 + 0.9t^4, & 0 \leq t \leq 20 \\ 1553800, & t \geq 20 \end{cases} \tag{19}$$

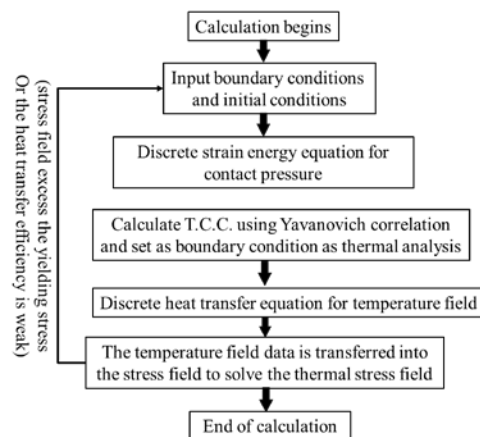


Fig. 4. Analysis procedure

ANALYSIS PROCEDURE

This paragraph depicts the simulation process. First, assume that there is no thermal resistance between the interfaces, the bring in the set temperature and stress boundary conditions. This step allows us to get contact pressure on the contact surface. Subsequently, the Yovanovich correlation was used to bring contact pressure into the contact thermal conductivity. Finally, touch thermal conductivity is introduced into the thermal analysis of finite elements as a new boundary condition. After obtaining the temperature field, it is brought into the stress analysis to obtain the thermal stress field in all directions. It is assumed that the initial boundary conditions are designed to make the stress field exceed the strength or heat. When efficiency is poor, it will jump back to the first step to set the boundary conditions to redesign, as shown in Figure 4.

RESULTS AND DISCUSSION

The finite element method is used to simulate transient one-dimensional heat transfer and two-dimensional stress annular fin tubes. Eight quadrilateral elements were used. The element distribution diagram is shown in Figure 5. The inner tube bundle is straight. The simulation was conducted for different contact thermal conductivities. The goal was to obtain the overall temperature and stress distribution, investigate the temperature spacing of the contact thermal conduction on the contact surface, and compare the variances in fin efficiency between steady states.

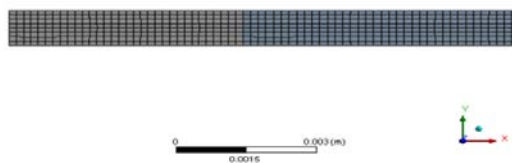


Fig. 5. Element arrangement of the analysis structure

The heat transfer analysis of the two-dimensional fins of Mustafa (2011) considering thermal contact conductivity is used as the simulation verification. The simulation results can be seen in Table 4, and the heat transfer amount and actual analytical solution calculated by the set software ANSYS can be seen. The resulting heat transfer error is extremely low. The purpose of this simulation is to confirm that the analysis process is correct when the fin boundary conditions have contact thermal conductivity.

Temperature Difference Analysis with or without Interference and Thermal Resistance

In the ideal state, since the interface assumes no contact thermal resistance, there is no energy loss when heat is transferred from one object to another. Accordingly, the heat flux and temperature distribution of the two interfaces are continuous. However, in actual cases, the heat will follow the nature of the interface, and the contact pressure has a certain loss. Figures 6 and 7 show the temperature distribution and enlarged view of materials in the interface with thermal resistance and no thermal resistance. The overall temperature change curve is close to the fin end and the temperature distribution. Moving to the lower right corner shows that the fin temperature decreases with position. The difference between the temperature and the interface temperature is related to the material properties and interface contact conditions.

Table 4. Comparison of heat transfer results with the numerical results.

$h(W/m^2K)$	K	$q(W)[7]$	q_{ANSYS}	$E_r(\%)$
100	0.24094	20.72	20.715	0.024
500	0.24094	37.30	37.29	0.026
1000	0.24094	42.10	42.103	0.007
5000	0.24094	48.58	48.584	0.008
100	0.96076	20.99	20.993	0.014
500	0.96076	38.34	38.339	0.002
1000	0.96076	43.67	43.667	0.006
5000	0.96076	52.17	52.174	0.007
100	2.0	21.00	21.008	0.038
500	2.0	38.40	38.39	0.026
1000	2.0	43.76	43.762	0.004
5000	2.0	52.44	52.45	0.076

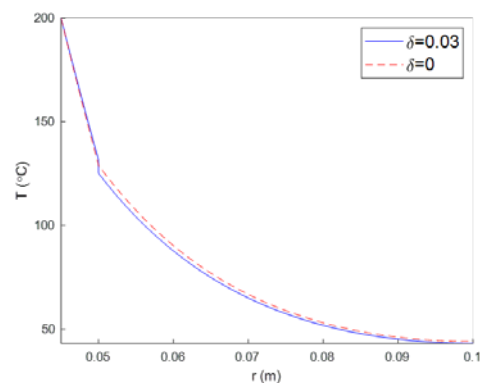


Fig. 6. Temperature field of aluminum fins with and without thermal contact resistance (fin radius ratio 1:1, $t=70$ sec)

In addition, the temperature difference on the interface will change over time. Figure 8 illustrates the relationship between temperature and position at various time points when copper is used, the ratio of internal and external radius is 1:1, and the interference is 0.03 mm. The temperature gradually increases with time. The temperature distribution display system, which is slowly approaching $t=70$,

gradually becomes steady state. As shown in Table 5, the interface temperature distinction is gradually increased from $t=5$ to $t=20$, and the receiver is gradually reduced from $t=20$ to $t=70$ because the effect of thermal resistance is amplified as the inner tube temperature rises until the inner tube is maintained at the same temperature. The heat transfer state tends to be warm, and the temperature difference of the interface will gradually decrease.

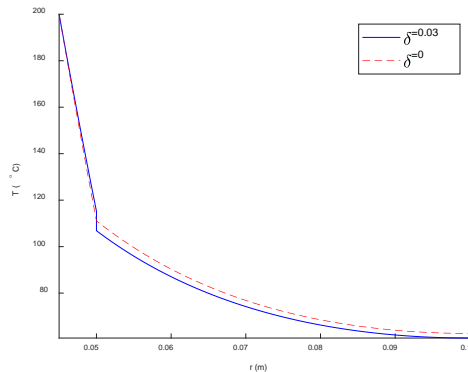


Fig. 7. Temperature field of copper fins with and without thermal contact resistance (fin radius ratio 1:1, $t=70$ sec)

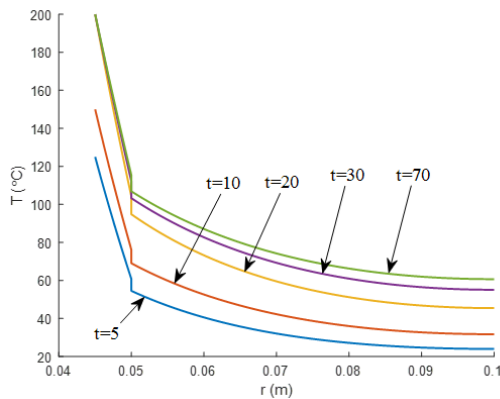


Fig. 8. Temperature field of copper fins at different time points (fin radius ratio 1:1, $\delta=0.03$ mm)

Table 5. Temperature difference of copper fins at varying time points (fin radius ratio 1:1, $\delta=0.03$ mm)

Time(sec)	Temperature difference(°C)
t=5	6.22
t=10	7.037
t=20	9.217
t=30	8.67
t=70	8.36

Analysis of Temperature Difference Between Interference and Fin Radius Ratios

First, two materials were selected to discuss the influence of disparate interference quantities on the temperature difference. The inner and outer diameter ratios were selected as a 1:1 condition. Figures 9 and

10 show temperature distribution maps at assorted time points. Tables 6 and 7 show that the temperature difference varies with time, and the temperature gradually increases from the beginning until $t=20$ seconds, mainly due to the influence of temperature boundary conditions. The inner tube temperature is raised from the first 100°C to 200°C at $t=20$ seconds, so the temperature difference will gradually decrease as the system temperature tends to maintain a steady state.

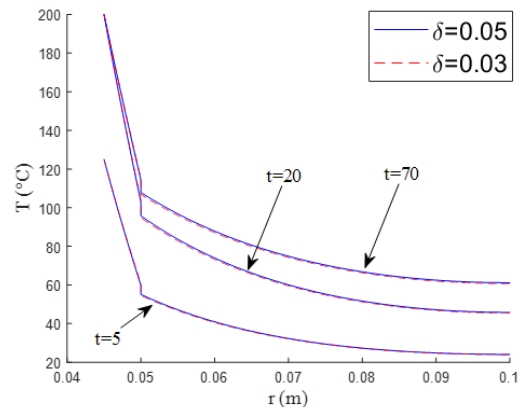


Fig. 9. Temperature field of copper fins with different interferences (fin radius ratio 1:1)

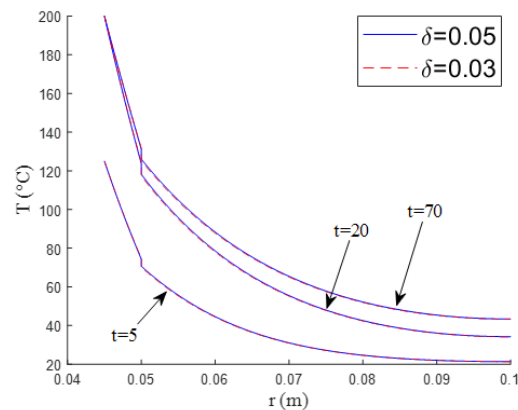


Fig. 10. Temperature field of aluminum fins with varying interferences (fin radius ratio 1:1)

Table 6. Temperature distinction of copper fins with varying interference (fin radius ratio 1:1)

Time(sec)	$\delta=0.03$ mm	$\delta=0.05$ mm
t=5	6.22	4.682
t=10	7.037	5.348
t=20	9.217	7.006
t=30	8.67	6.58
t=70	8.36	6.35

In addition, no matter what kind of material, the smaller the interference amount, the smaller the temperature difference of the interface. The larger the interference amount, the larger the contact pressure of

the interface, and the contact pressure is proportional to contact thermal conductivity. Accordingly, regarding contact, the higher the thermal conductivity, the better the heat transfer property of the interface. When the heat transfer property of the interface is better, heat energy is effectively transmitted. When the heat transfer of the interface is worse, heat will accumulate in the inner tube. The tube temperature is higher, and the fin temperature is lower.

Table 7. Temperature disparity of aluminum fins with distinct interferences (fin radius ratio 1:1)

Time(sec)	$\delta=0.03$ mm	$\delta=0.05$ mm
t=5	4.619	3.594
t=10	5.183	4.06
t=20	6.93	5.43
t=30	6.59	5.16
t=70	6.49	5.08

The receiver selects two materials to discuss the effect of inner and outer diameter ratios on the temperature distinction. See figures 11 and 12. The interference was 0.05 mm at t=70 seconds. The internal/outer diameter ratio here is that the length of the outer diameter of the inner tube is longer than the inner diameter to the outer diameter of the upper fin. As shown in tables 8 and 9, the smaller the ratio of the inner and outer diameters, the smaller the temperature variation of the interface; however, the amplitude is not large. When the scale becomes larger, the contact pressure will also increase, but the temperature difference caused by the small-scale change is not obvious. It is speculated that when the scale change is much larger than 1:1, the temperature differential can cause a more significant difference. The inconsistent scale causes various heat transfer spaces, which leads to different temperature distributions when the overall model reaches a steady state. Due to the relationship between the fin end insulation, if the fin scale is smaller, the heat flow will hinder the lead time and lead to the overall mode. The shape temperature distribution is increased.

Thermal Stres Analysis of Divergent Interferences

Two different materials were selected to discuss the influence of different interference on the radial stress. The fin radius ratios were selected as 1:1 conditions, and the discussion time point was close to the steady state of t=70 seconds.

1. It can be seen from Figure 13 to Figure 14 that the stress distribution of the ideal state (without considering the amount of interference and thermal resistance) is significantly lower than the other two sets of data at the interface, due to the interface inutility under ideal conditions. There is no pre-stress in the condition, so when the fin temperature rises and expands, the contact pressure of the interface will loosen

slightly with the thermal expansion of the fin. In addition, the interface stress will vary when the materials are different. The degree of influence depends on the temperature disparity between the two interfaces and the thermal expansion coefficient of the two interface materials.

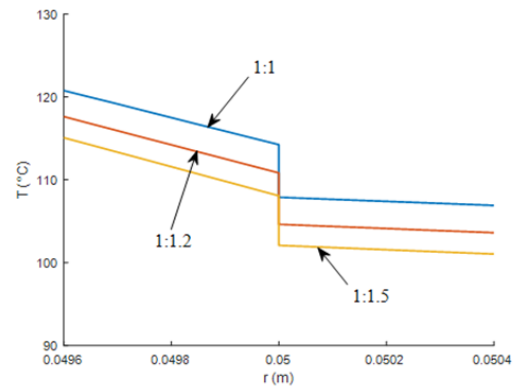


Fig. 11. Temperature field of copper fins with different fin radius ratios (t=70 sec, $\delta=0.05$ mm)

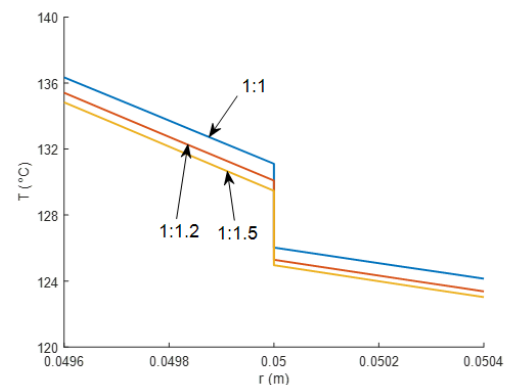


Fig. 12. Temperature field of aluminum fins with different fin radius ratios (t=70 sec, $\delta=0.05$ mm)

2. The stress distribution is smoother when the inner tube has an interference amount, which is also because the heat transfer is poorer than the ideal state, and the inner tube temperature is higher than the actual state in the ideal state and the fin. The ideal inner diameter of the sheet is lower than the actual state, thus causing a difference in the degree of thermal expansion. When the amount of interference is large, the contact pressure is large, so the interference force is greater than 0.03 mm when the interference amount is 0.05 mm.
3. When the amount of interference is small, the number of sudden drops in the stress value of the inner tube interface is large. Presumably, the degree of thermal expansion between the two materials is inconsistent, the coefficient of thermal expansion of the inner tube is small, and the coefficient of the thermal expansion of

the fin is large, so the temperature rises. The expansion of the tube is smaller than that of the fin, and the small interference means that the contact pressure is small, so a small amount of stress is reduced near the inner tube. Otherwise, when the interference amount is large, the contact pressure is large, so the inner tube is close to the interface. A relatively continuous stress distribution is produced.

Table 8. Temperature difference of copper fins with different fin radius ratio (t=70 sec、δ=0.05 mm)

Time (δ=0.05 mm)	Fin radius ratio (1:1)	Fin radius ratio(1:1.2)	Fin radius ratio (1:1.5)
t=5	4.682	4.466	4.294
t=10	5.348	5.085	4.795
t=20	7.006	6.734	6.398
t=30	6.58	6.39	6.125
t=70	6.35	6.2	5.98

Table9. Temperature difference of aluminum fins with different fin radius ratio (t=70 sec、δ=0.05 mm)

Time (δ=0.05 mm)	Fin radius ratio (1:1)	Fin radius ratio(1:1.2)	Fin radius ratio (1:1.5)
t=5	3.594	3.4	3.227
t=10	4.06	3.794	3.546
t=20	5.43	5.1	4.77
t=30	5.16	4.86	4.56
t=70	5.08	4.8	4.51

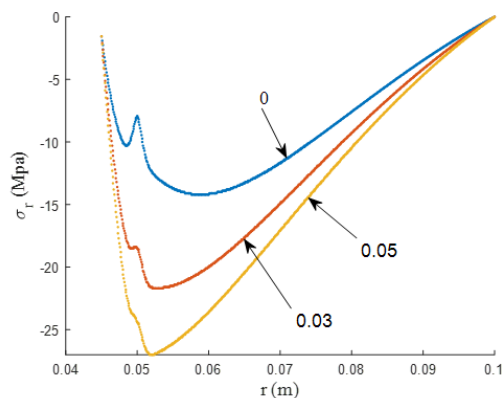


Fig. 13. Radial stress field of copper fins with varying interferences (fin radius ratio 1:1, t=70 sec)

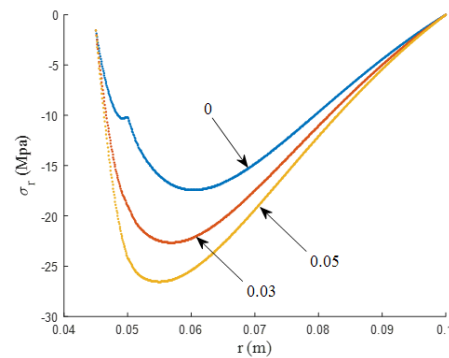


Fig. 14. Radial stress field of aluminum fins with varying interferences (fin radius ratio 1:1, t=70 sec) The receivers explore the effects of disparate interferences on circumferential stress under the same geometry and boundary conditions.

1. In figures 15 to Fig. 16 the circumferential stress. The values are the tensile force from the compression force of the inner diameter of the fin to the outer diameter of the fin, and the ideal state (regardless of the amount of interference, heat is not considered). The resistance of the inner diameter is larger than the actual state, and the tensile force at the end is smaller than the actual state. The trend is the heat of the hollow sheet in the inner diameter of the fin and heat flux. The stress analysis is the same.

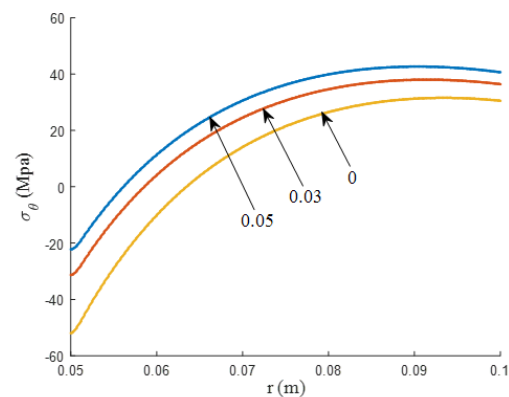


Fig. 15. Circumferential stress field of copper fins with varying interferences (fin radius ratio 1:1, t=70 sec.)

- It is presumed that the smaller the degree of preloading of the inner ring, the smaller the radial displacement of the overall model. According to Hooke's law $\sigma_\theta = \frac{E}{1-\nu^2} \left(\frac{u}{r} + \nu \frac{\partial u}{\partial r} - (1+\nu)\alpha T \right)$, when the effect caused by the temperature change is less than the effect caused by the displacement, the circumferential direction stress will exhibit compressive forces and vice versa.
- In addition, when the amount of interference is small, the circumferential compressive stress

value of the fin base is large and the value is closer to the steady state with time. This is known according to Hooke's law, when the amount of interference is large. The radial displacement is also larger, so when the effects of temperature $(1+\nu)\alpha T$ are similar, the radial displacement amount causes the circumferential stress value to be small.

Thermal Stress Analysis of Divergent Radius Ratios of Annular Fins

The influence of the ratio of fin radii on radial stress was selected for $\delta=0.05$ mm. Since the difference in interferences in the previous paragraph was found, the pressure of the interface was changed when the copper alloy was selected. Therefore, the material is selected as copper was used for analysis.

1. Figures 17 to 19 reveal the relationship between the radial stress and the position of different internal and external diameter ratios under the same interference amount. Although the interference amount is identical, the difference in the inner and outer diameter ratios will cause distribution in the stress field's distribution. The disparity in size and the larger the ratio of the inner and outer diameters, the greater the value of the radial compressive stress. This is because the stiffness of the material is larger as the ratio of the inner and outer diameters is larger, so a larger radial compressive stress is required to overcome the same amount of interference.

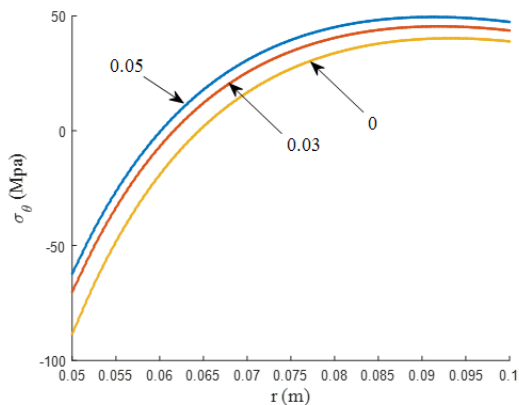


Fig. 16. Circumferential stress field of aluminum fins with varying interference (fin radius ratio 1:1, $t=70$ sec.)

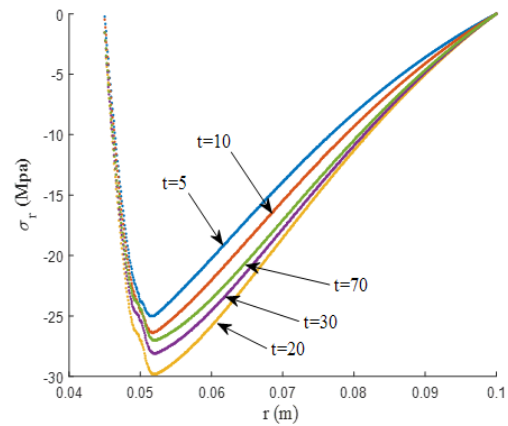


Fig. 17. Radial stress field of copper fins at assorted time points (fin radius ratio 1:1, $\delta=0.05$ mm)

2. The figure also reveals that the stress value before $t=20$ will gradually increase with time, and the stress value will decrease after $t=20$ due to the boundary condition. The boundary condition is maintained after $t=20$. At a constant pressure, the system will gradually become steady state, and the radial stress will decrease due to the slower temperature distinction of the interface.

The effect of varying fin radius ratios on circumferential stress is discussed under the same geometry and boundary conditions.

1. Figures 20 to 22 show the difference in circumferential stress between the same interference amount at a range of inner and outer diameter ratios. The larger the ratio of the inner and outer diameters, the greater the circumferential stress value of the fin base. Since the model stiffness value is larger as the ratio of the inner and outer diameters is larger, the larger the compressive stress required to achieve the equivalent interference amount. In addition, the magnitude of the circumferential stress will also increase with time, which is because the contact pressure of the interface will increase with the external force and heat as time passes. The radial displacement is also followed according to the above inference. It becomes larger, thus causing circumferential stress to enlarge.

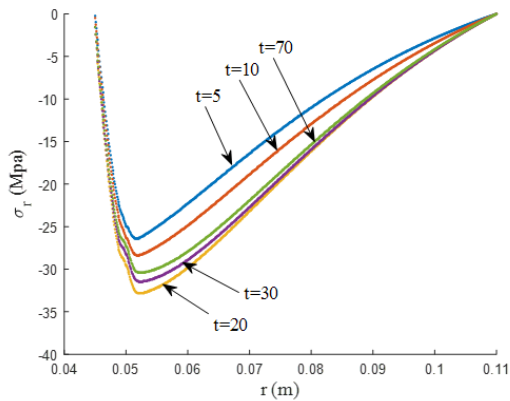


Fig. 18. Radial stress field of copper fins at disparate time points (fin radius ratio 1:1.2, $\delta=0.05$ mm)

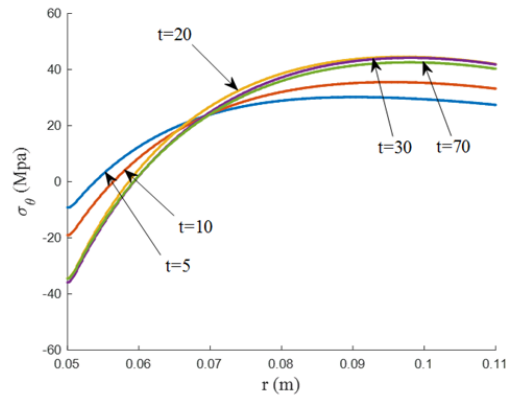


Fig. 21. Circumferential stress field of copper fins at different time points (fin radius ratio 1:1.2, $\delta=0.05$ mm)

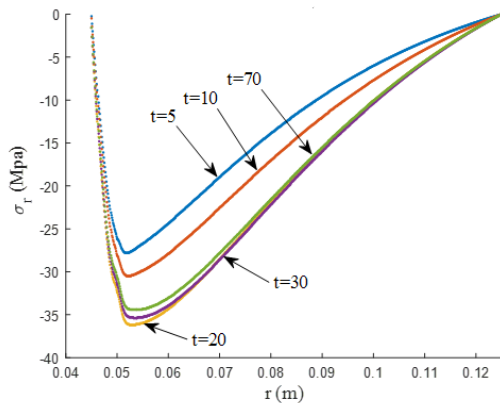


Fig. 19. Radial stress field of copper fins at diverse time points (fin radius ratio 1:1.5, $\delta=0.05$ mm)

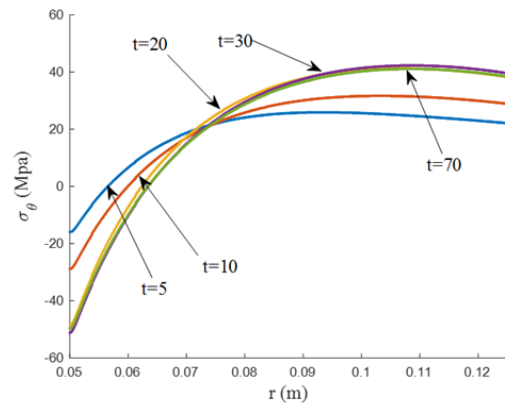


Fig. 22. Circumferential stress field of copper fins at distinct time points (fin radius ratio 1:1.5, $\delta=0.05$ mm)

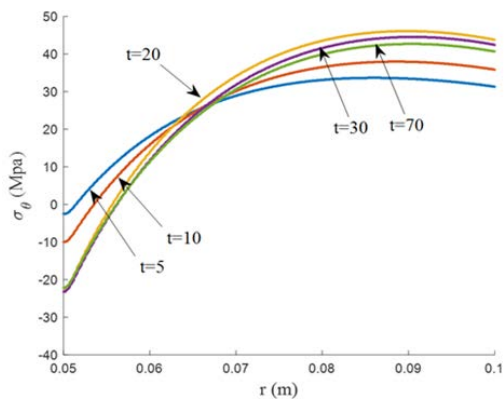


Fig. 20. Circumferential stress field of copper fins at different time points (fin radius ratio 1:1, $\delta=0.05$ mm)

Comparison of Maximum Equivalent Stress for Fin Safety Factor

Tables 10 and 11 demonstrate the maximum equivalent stress and fin safety factor of copper and aluminum at different ratios of inner and outer diameters and varying interferences, respectively, can be seen regardless of the material when the interference is zero. The maximum equivalent stress is the maximum value. Although the radial thermal stress value is the lowest when the interference is zero, the circumferential stress value is the largest, and the value is much larger than the interference amount. This is because the calculation is maximum. The effect force time variable contains the stress values in all directions, so this situation is caused; therefore, the amount of interference should be considered when designing the fins. The table illustrates that the maximum equivalent stress without interference is significantly overestimated.

$$\text{The safety factor is defined as } S.F. = \frac{\sigma_{Mises}}{\sigma_Y},$$

where σ_Y represents the yielding stress of the material and σ_{Mises} the maximum equivalent stress.

It can be seen from both tables that the safety factor is less than 1, and it is shown that the fins are safe under the designed interference amount. Later, in the design of the fins, the method can also be used to preliminarily determine whether there will be material fluctuation under different interference quantities. If the stress field exceeds the drop strength, the interference amount, material properties and fin size can be used.

Table 10. Copper fin safety factor for all cases

Material	Fin radius ratio	δ	σ_{Mises}	σ_Y	S.F.
Cu	1:1	0	49.3	280	0.176
Cu	1:1	0.03	28.1	280	0.100
Cu	1:1	0.05	24.3	280	0.086
Cu	1:1.2	0	59.2	280	0.211
Cu	1:1.2	0.03	38.3	280	0.136
Cu	1:1.2	0.05	32.7	280	0.116
Cu	1:1.5	0	71.7	280	0.256
Cu	1:1.5	0.03	51.1	280	0.182
Cu	1:1.5	0.05	44.7	280	0.159

Pressure unit: Mpa

Table 11. Aluminum fin safety factor for all cases

Material	Fin radius ratio	δ	σ_{Mises}	σ_Y	S.F.
Al	1:1	0	84.5	280	0.302
Al	1:1	0.03	63.4	280	0.226
Al	1:1	0.05	55.0	280	0.196
Al	1:1.2	0	93.3	280	0.333
Al	1:1.2	0.03	73.3	280	0.262
Al	1:1.2	0.05	65.2	280	0.233
Al	1:1.5	0	103.5	280	0.370
Al	1:1.5	0.03	84.1	280	0.301
Al	1:1.5	0.05	76.3	280	0.273

Pressure unit: Mpa

CONCLUDING REMARKS

This paper proposes, the theory and finite element analysis simulation and flow of the relevant contact thermal conductivity of the annular fin with inner tube contact. The fin's temperature distribution, heat dissipation efficiency, thermal stress field, and safety factor are analyzed by the above, and the results are as follows.

1. Contact pressure is directly proportional to contact thermal conductivity. Contact thermal conductivity as a boundary condition will change with time. Therefore, when analyzing the interference fit fin problem, transient analysis is needed.
2. Contact pressure affects the contact thermal conductivity, and the contact thermal conductivity influences the heat dissipation and efficiency of the fin. Therefore, as a more complete design analysis, the ratio of the inner and outer diameter, interference amount,

material, interface condition, etc. should be considered. The conditions directly affect heat dissipation performance.

3. The temperature difference on the contact surface will decrease as the contact pressure increases. The interference amount can effectively reduce the temperature difference. However, if the interference amount is too large, the material itself may be degraded. Therefore, thermal stress analysis is necessary.
4. From the simulation results, the magnitude of the stress field is related to the interference amount, the ratio of the inner and outer diameters, and the thermal expansion rate of the material. The larger the interference amount, the smaller the σ_{θ} is near the contact surface and the larger the σ_r , and inner tube radius and fin, the greater the sheet-length-to-size ratio, the greater the stress in both directions.
5. When the safety factor is less than 1, the display is safe under the interference of the design. Later, in the design of the fins, the method can also be used to preliminarily determine whether there will be material fluctuation under disparate interference quantities. If the stress field exceeds the yielding strength, the interference amount, material properties and fin size can be modified and enhanced to suit the design object.

ACKNOWLEDGMENT

Financial support for this work was provided by the Ministry of Science and Technology of Taiwan under the contract MOST 105-2221-E-006-004

REFERENCES

- Aziz, A., "Periodic Heat Transfer in Annular Fins," *J. Heat Transfer*, Vol. 97, No. 2, pp.302-303(1975).
- Chiu, C.H., Chen, C. K., "Application of The Decomposition Method to Thermal Stresses in Isotropic Circular Fins with Temperature-dependent Thermal Conductivity," *Acta Mechanica*, Vol. 157, No. 1, pp. 147-158(2002).
- Duan S.P., Wu Q.S., "Analysis of various processing techniques of finned tubes." *Water conservancy and electric power machinery*, Vol.6 (1999).
- Jabbari, M., Sohrabpour, S., Eslami, M.R., "Mechanical and Thermal Stresses in a Functionally Graded Hollow Cylinder due to Radially Symmetric Loads," *International Journal of Pressure Vessels and Piping*, Vol. 79, No. 7, pp. 493-497(2002).

- Kang, H.S., Look Jr., D.C., "Two Dimensional Trapezoidal Fins Analysis," *Computational Mechanics*, Vol. 19, No. 3, pp.247-250(1997).
- Look Jr., D.C., "Fin on a Pipe (Insulated Tip): Minimum Conditions for Fin to Be Beneficial," *Heat Transfer Engineering*, Vol. 16, No. 3, pp. 65-75(1995).
- Look Jr., D.C., "1-D Fin Tip Boundary Condition Corrections," *Heat Transfer Engineering*, Vol. 18, No. 2, pp. 46-49(1997).
- Look Jr., D.C., "1-D Fin Tip Boundary Condition Corrections," *Heat Transfer Engineering*, Vol. 18, No. 2, pp. 46-49(1997).
- Mikić, B.B., "Thermal Contact Conductance: Theoretical Considerations," *International Journal of Heat and Mass Transfer*, Vol. 17, No. 2, pp. 205-214,(1974).
- Mustafa, M.T., Zubair, S. M., Arif, A. F. M., "Thermal Analysis of Orthotropic Annularfins with Contact Resistance: A Closed-form Analytical Solution," *Applied Thermal Engineering*, Vol. 31, No. 5, pp. 937-945(2011).
- Shuja, S.Z., Zubair, S.M., Khan, M.S., "Thermoeconomic Design and Analysis of Constant Cross-sectional Area Fins," *Heat and Mass Transfer*, Vol. 34, No. 5, pp. 357-364(1999).
- Ullmann, A., Kalman, H., "Efficiency and Optimized Dimensions of Annular Fins of Different Cross-section Shapes," *International Journal of Heat and Mass Transfer*, Vol. 32, No. 6, pp. 1105-1110(1989).
- Wu, S.S., "Analysis on Transient Thermal Stresses in an Annular Fin," *Journal of Thermal Stresses*, Vol. 20, No. 6, pp. 591-615 (1997).
- Yovanovich, M.M., Culham, J.R., Lemczyk, T.F., "Simplified Solutions to Circular Annular Fins with Contact Resistance and End Cooling," *Journal of Thermophysics and Heat Transfer*, Vol. 2, No. 2, pp. 152-157(1988).
- Yovanovich, M.M., "New Contact and Gap Conductance Correlations for Conforming Rough Surfaces," *AIAA 16th Thermophysics Conference, Palo Alto, CA*, No. 81-1164(1985).
- Yu, L.T., Chen, C.K., "Application of the Taylor Transformation to the Transient Temperature Response of an Annular Fin," *Heat Transfer Engineering*, Vol. 20, No. 1, pp. 78-87(1999).
- Yovanovich, M.M., "Four Decades of Research on Thermal Contact, Gap, and Joint Resistance in Microelectronics," *IEEE*

Transactions on Components and Packaging Technologies, Vol. 28, No. 2, pp. 182-206(2005).

Yüncü, H., "Thermal Contact Conductance of Nominally Flat Surfaces," *Heat and Mass Transfer*, Vol. 43, No. 1, pp. 1-5(2006).

環形鰭片在不同接觸壓力 與熱導下之熱應力分析

賴新一 魏任宏 陳朝光
國立成功大學機工程學系

張桂豪
國立成功大學產學創新總中心

摘要

本文旨在探討傳送飽和水蒸汽之變溫內管與其外在具干涉之環型鰭片在不同接觸壓力下之熱傳遞與熱應力問題。主要相關變量包括鰭片、內管表面干涉量、鰭片材質與內外徑比，上述可用來求取不同變量下之溫度與熱應力分布；及考量超出設計上限所帶來之可能破壞，以確認系統能在安全設計內範疇下運作。

首先考慮無熱阻情形下並給予內管壁一隨時間變化之溫度邊界條件與該溫度下之飽和水蒸汽壓，求解得兩介面之接觸壓力，接者利用 Yovanovich 經驗式換算出接觸熱導，再以接觸熱導作為鰭片之邊界條件求解其溫度分布曲線，並利用溫度場求得熱應力分布曲線，包含徑向應力與切向應力。文中探討不同干涉量及不同內外徑比對於鰭片之溫度分布、介面溫差、熱應力分布之影響，以及穩態時之鰭片熱傳效率與熱傳量之關係。

研究結果得知，接觸壓力影響接觸熱導，而接觸熱導影響鰭片熱傳效率。又接觸面上之溫差會隨著接觸壓增大而變小，干涉量可有效地縮小溫度差距且應力場大小會隨著干涉量、內外徑比與其本身材料熱膨脹率而變化。干涉量越大接觸面附近徑向應力越大，而周向應力分布為鰭片基底之壓所力轉換成鰭片尾端之拉伸力，這是由於當溫度變化所造成的效應小於位移所造成的效應時，周向應力會呈現壓縮力，反之則會呈現拉伸力。又內外徑比越大對於周向與徑向之應力都會越大。